

Electrochemical performance of nickel/ metal hydride batteries under unconventional conditions and degradation analysis^①

LI Li(李 丽), WU Feng(吴 锋), YANG Kai(杨 凯), WANG Jing(王 敬), CHEN Shi(陈 实)
(School of Chemical Engineering and Environmental Science, Beijing Institute of Technology,
National Development Center of Hi-Tech Green Materials, Beijing 100081, China)

Abstract The charge-discharge performance and cycle stability of D size Ni/MH batteries at -20 °C, 25 °C and 55 °C were examined. The results show that the decline rate of Ni/MH battery discharge capacity at -20 °C and 55 °C are 12.1% and 13.6%, and the average discharge voltage decreases by a value of 0.13 V and 0.06 V respectively, cycling stability declines obviously at various temperatures. The capacity degradation of Ni/MH batteries under low temperature is reversible, belonging to transient degradation and that of high and normal temperatures are not reversible, belonging to permanent degradation. Electrochemical impedance spectroscopy, scanning electron microscope and energy dispersive X-ray analyzer were introduced to study the main causes of cycling deterioration of Ni/MH batteries.

Key words: Ni/MH battery; electrode materials; degradation; cycle life

CLC number: TM 912

Document code: A

1 INTRODUCTION

Since the beginning of 1990s, the nickel/ metal hydride (Ni/MH) secondary batteries have been extensively applied in various consumer and portable electronic fields, especially in battery-powered electric vehicles (EV) or hybrid electric vehicles (HEV), because of their higher energy density, higher capacity, longer cycle life and more friendly environment than the conventional nickel/cadmium battery^[1-3]. The volume energy density for Ni/MH batteries has doubled from 180 Wh·L⁻¹ in 1990 to 360 Wh·L⁻¹ in 1997, a value comparable to that for lithium-ion battery, as shown in Fig. 1^[4]. However, the applications of Ni/MH batteries are limited under some special conditions, such as extreme torridity or chilliness environments, military secondary planet and soldier equipments. The performance of the battery is degraded seriously under these extremely unconventional conditions. At present, high and low-temperature characteristics of Ni/MH batteries are improved from the following aspects: 1) optimization of the electrolyte composition and concentration; 2) treatment of the positive and negative electrodes, such as using additives or surface modification; 3) replacement of polyolefin separator with nylon separator.

About the degradation mechanism of Ni/MH batteries, Willems^[5] studied that the cause of capaci-

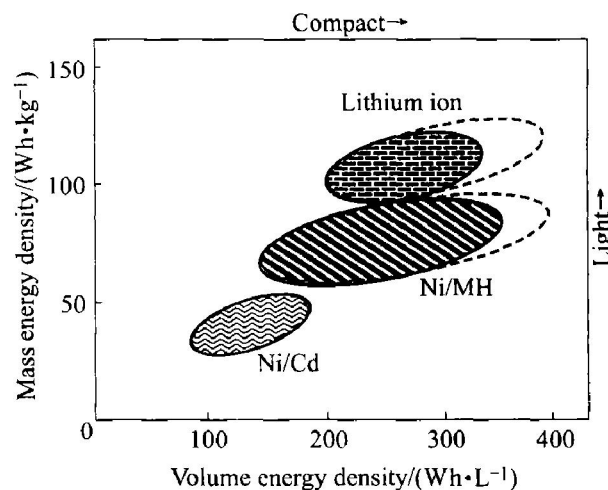


Fig. 1 Energy density per volume and mass for small rechargeable batteries

ty decline attributed to the crystal lattice expansion and pulverization of the hydrogen storage alloy. Boonstra et al^[6] showed that the formation results in the capacity decrease of La(OH)₃ and Ni(OH)₂. XIA et al^[7] showed that the main causes for the degradation of Mm alloy hydride electrodes were the increase of internal stress, the expansion of crystal lattice and the preferential dissolution of Mm, rather than the oxidation of the alloy. Emphasis was put on revealing the electrochemical performance and degradation mechanism of Ni/MH batteries at high and low temperature

① **Foundation item:** Project(2002CB211800) supported by National Key Basic Research and Development Program and project(2001CCA05000) supported by National Key Program for Basic Research of China

Received date: 2003 - 03 - 18; **Accepted date:** 2003 - 05 - 28

Correspondence: WU Feng; Tel: + 86-10-68912508; Fax: + 86-10-68451429; E-mail address: wufeng863@vip.sina.com

systemically.

2 EXPERIMENTAL

2.1 Preparation of electrodes and Ni/MH batteries

Hydrogen storage alloy $M\text{Ni}_{3.6}\text{Co}_{0.7}\text{Mn}_{0.4}\text{Al}_{0.3}$ (where Ml denotes La-rich mischmetal consist of 64.6% La, 5.9% Ce, 26.6% Pr and 2.2% Nd) prepared by induction melting with a stoichiometric mixture of Ml, Ni, Mn, Al and Co, followed by the annealing process at 1 000 °C. Then, the alloy ingot was mechanically pulverized to 74 μm . The alloy powder had been immersed into 6 mol/L KOH solution at 70 °C for 18 h. The negative electrode of Ni/MH battery was formed with the mixture of alloy powder, a small amount of nickel and 3% polytetrafluoroethylene (PTFE) which were pressed into nickel foam substrate. Positive electrode was prepared with filling a nickel foam substrate with the mixture of $\text{Ni}(\text{OH})_2$, CoO and PTFE. A non-woven polypropylene separator was inserted between the positive and negative electrodes, and then spirally was rolled into D-type cylindrical battery cans. Mixed solution with 7 mol/L KOH and 1 mol/L LiOH as electrolyte was injected and then the batteries were sealed.

2.2 Measurements of electrochemical performance of Ni/MH batteries

Testing the charge-discharge cycle was carried out with the scheme that consisted of a charge with 1 C for 1.5 h, a pause for 10 min, and a discharge with 1 C to 1.0 V after charge-discharge activation at low rate (0.1 C). The cycle life of the battery was defined by the cycle number, it was considered as failure when the discharge capacity decreased to 80% of the original capacity.

The charge-discharge experiments and cycle life tests were performed by an Arbin apparatus, controlled by an external computer.

The equipment for electrochemical impedance spectroscopy (EIS) consists of a M273 Potentiostat/Galvanostat and a M3501A Lock-in Amplifier controlled by a personal computer. The EIS experiments were conducted after a number of desired charge-discharge cycles. The impedance data were obtained in the range of 0.05 - 10 000 Hz. The amplitude of the modulated signal was 10 mV.

Scanning electron microscopy (SEM) and energy dispersive X-ray analyzer (EDAX) were carried out with a JSM model 6 400 scanning electron microscope equipped with a Noran F-2 EDX unite. Then the original changes in surface morphology of positive and negative electrodes were examined.

3 RESULTS AND DISCUSSION

3.1 Studies of electrochemical performance of Ni/MH batteries under unconventional conditions

For comparison, it was defined that:

$$R = \frac{C_0 - C_t}{C_0} \times 100\%$$

where R is the capacity degradation rate of the Ni/MH batteries at different temperatures; C_0 is the discharge capacity at 25 °C; C_t is the discharge capacity at - 20 °C - 55 °C.

The discharge voltage of D size sealed-type Ni/MH batteries as the discharge capacity at different temperatures (- 20 °C, 25 °C and 55 °C) are shown in Fig. 2. It can be observed that the capacity degradation rate of Ni/MH batteries at - 20 °C and 55 °C are 12.1% and 13.6% respectively. And at the same time, the corresponding discharge voltages decreased obviously with 0.13V and 0.06V respectively.

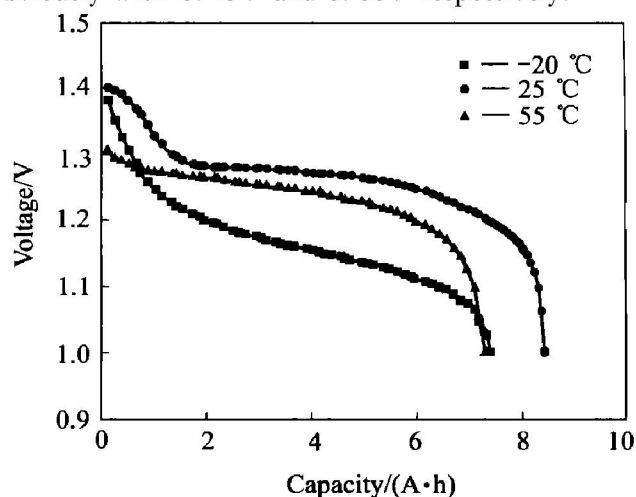


Fig. 2 D size Ni/MH battery discharge curve with 1C rate at different temperatures

Obviously, the characteristics of Ni/MH batteries at high and normal temperatures are superior to that of low temperature from Fig. 2. The main reason is that the higher temperature is beneficial to the diffusion of hydrogen in MH alloy, which can improve its dynamic performances.

The high-rate discharge ability (r) was defined as follows:

$$r = \frac{C_n}{C_1} \times 100\%$$

where C_1 and C_n represent the discharge capacity at 1C and n C respectively.

High-rate discharge curve of D size Ni/NH battery at various temperatures is shown in Fig. 3. To compare the high-rate discharge (HRD) at 10C discharge, it only decrease to 80% of the original capacity at 55 °C, and about to 40% at 25 and - 20 °C.

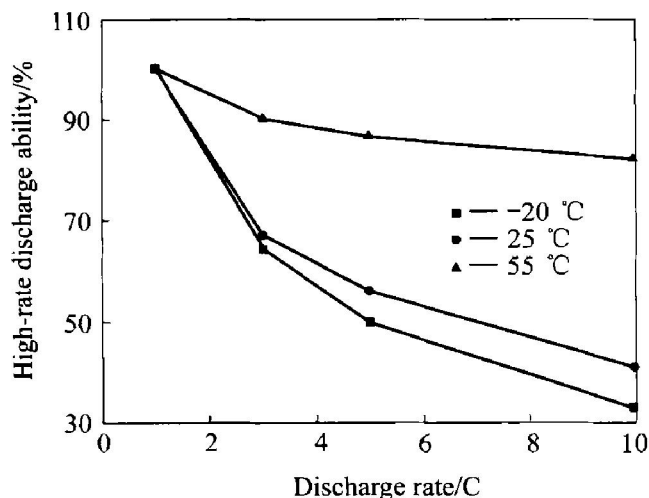


Fig. 3 High rate discharge curve of D size Ni/MH battery at various temperatures

The HRD characteristic of Ni/MH batteries at 25 °C is inferior to that at 55 °C, and superior slightly to that at -20 °C.

The discharge capacity of D size sealed type Ni/MH batteries as the number of charge-discharge cycle (n) at -20, 25 and 55 °C are shown in Fig. 4. It can be observed that, with the increasing of n , the discharge capacity of the battery at 25 °C ascended at first 300 times, and descended bit by bit till n is 750, then decayed until it reaches 80% of the original capacity at the 900th cycle. The battery is thus considered as failure. While the discharge capacity at -20 °C and 55 °C descended from the beginning of cycle. The speeds of discharge capacity at -20, 25 and 55 °C are 5.89, 2.42 and 9.97 mA·h every cycle respectively.

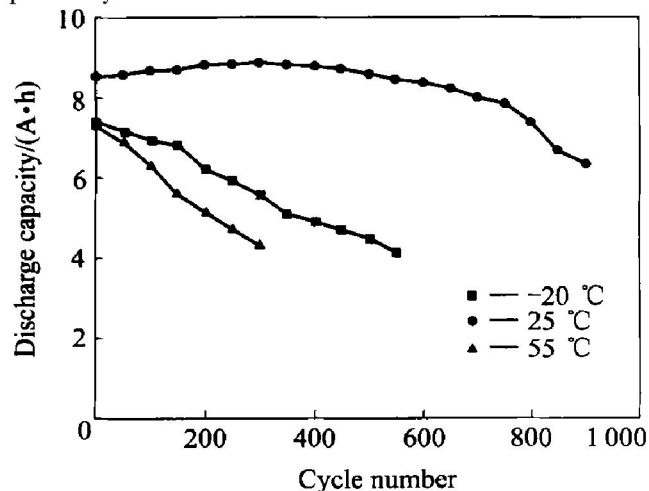


Fig. 4 Cycling stability curves of D size Ni/MH battery at different temperature

3.2 EIS studies of Ni/MH batteries during charge-discharge cycling

The typical Nyquist diagrams of the Ni/MH batteries are shown in Fig. 5. At high frequencies, the diagram starts with a semicircle and as the frequency

decreases, it changes to the straight line. The semicircle reflects the impedance of the electrochemical reaction of the battery, while the straight line indicates the diffusion of the electro-active species. Solution resistance was determined by the intersection point of the semicircle with the real axis, including the total ohmic resistance of the solution, the separator and the electrodes^[8]. According to the experiment conditions, the equivalent circuit of the Ni/MH battery is shown in Fig. 6 simply. And Table 1 is the fitting parameters of EIS for the batteries a, b, c and d.

The sequence from high to low of R_s , R_t and Z_w are d, b, c and a, and that of Q_c is a, c, b and

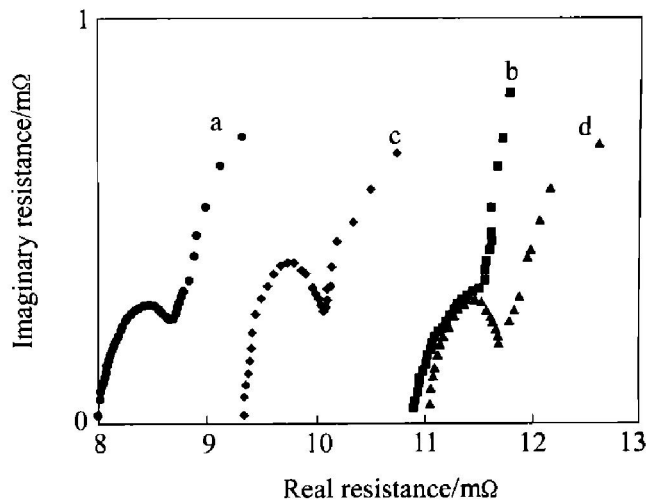


Fig. 5 Typical Nyquist diagrams of Ni/MH batteries

a—Before cycle; b—Failure battery at 25 °C; c—Failure battery at -20 °C; d—Failure battery at 55 °C

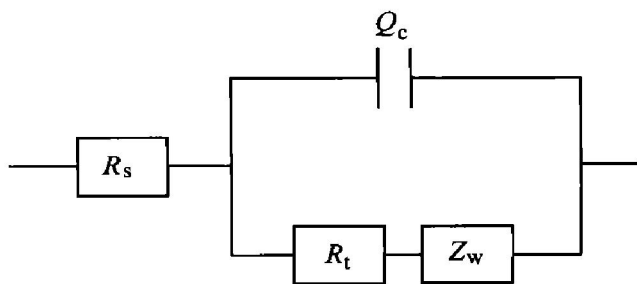


Fig. 6 Equivalent circuit of Ni/MH battery

R_s —Ohmic resistance of cell;
 R_t —Reactive resistance of cell;
 Q_c —Interface capacity of cell;
 Z_w —Warburg impedance of cell

Table 1 Fitting parameters of EIS for battery

Battery	$R_s / m\Omega$	$R_t / m\Omega$	Z_w / Ω	Q_c / F
a	8.032	0.300 2	10.29	76.28
b	10.930	0.507 8	19.56	50.79
c	9.305	0.381 4	18.01	55.48
d	11.010	0.622 9	21.33	38.22

d. It is indicated that the electrochemical performances were increased gradually in term of the sequence of d, b, c and a. The increase of R_s is mainly due to the drying out of the separator, and leads to the decrease of the discharge voltage. The increase of R_t on the surface of the electrodes would lead to the loss of electrochemical performance and the decrease of the capacity.

On the other hand, it can be observed from Table 1 that both R_s and R_t of the battery c increase slightly compared with the battery a. Because the voltage performance of the battery related to R_s , and battery capacity related to R_t ^[9], so we inferred that the degradation of the battery c was a superficial phenomenon. In order to validate this suspect inference, the discharge capacity tests of the battery a, b, c and d were performed at 25 °C again.

From Fig. 7, it is obviously observed that the

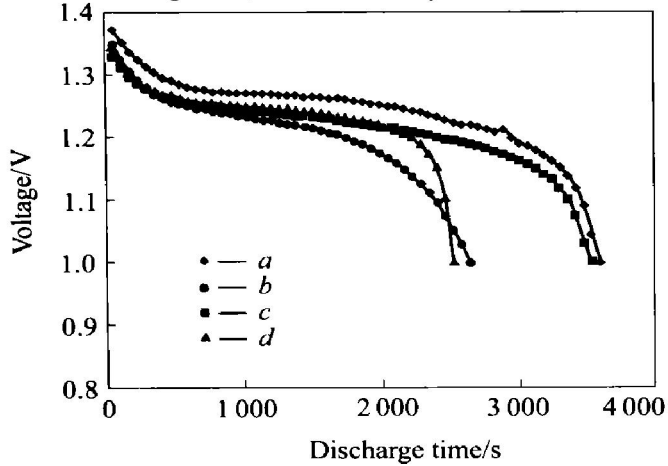


Fig. 7 Ni / MH battery discharge curve at 1C rate at 25 °C

discharge capacity of the battery c can be resumed at room temperature. This means that the capacity degradation of Ni/MH batteries under low temperature was reversible, belonging to transient degradation. While those of high and normal temperatures were not reversible, belonging to permanent degradation.

3.3 SEM-EDAX studies on structure of electrodes during charge-discharge cycling

In order to further investigate the mechanism of degradation, the sealed-type Ni/MH batteries were disassembled after the degradation for SEM studies. The positive and negative electrodes were taken out of the batteries and inspected by SEM and EDAX after washing and drying.

Fig. 8 shows that the surface morphology of the positive electrodes of the battery a, b, c and d. The particle size becomes smaller with the increasing of n because of the crystal lattice expansion of $\text{Ni}(\text{OH})_2$. The active materials scaled off from the electrode become more seriously with the increasing of the n and the rate of discharge. It is evident that the cracks of positive electrode are generated and become more and more serious. Meanwhile, the active materials powder block scale off from electrodes quickly. It had been demonstrated when the electrodes was cycled, the active material had significant changes in phase, oxidation state, hydration state, crystallinity and density, etc. These changes led to the gradual extrusion of the active material scaled off from the electrode substrate and fell into the electrolyte or the separator in the battery^[10], which caused the capacity decay of the positive electrode.

It can be seen over the lifetime of different

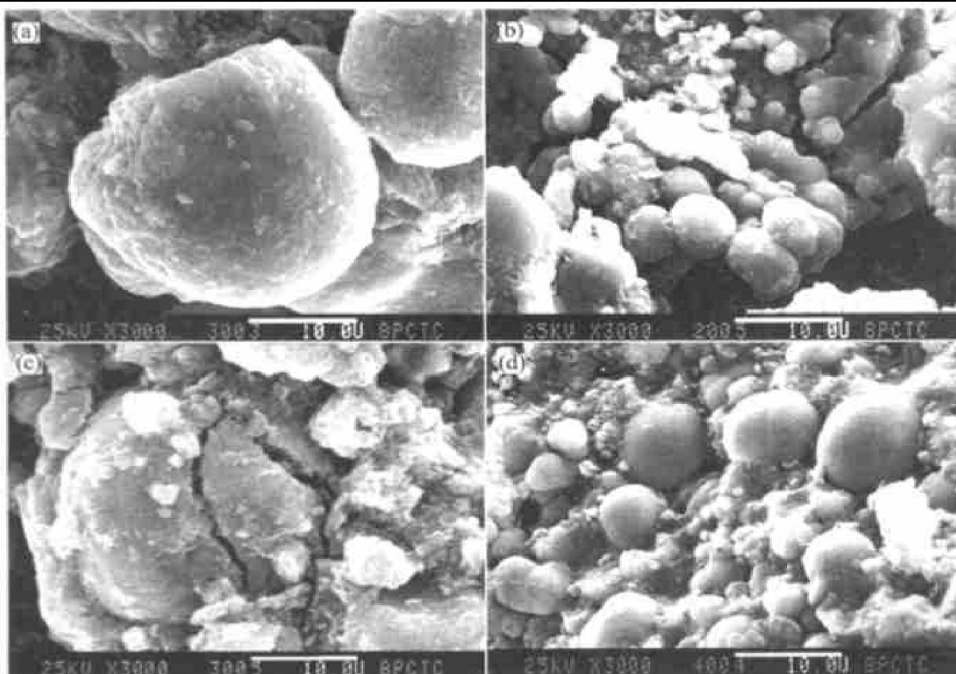


Fig. 8 SEM images of positive electrode

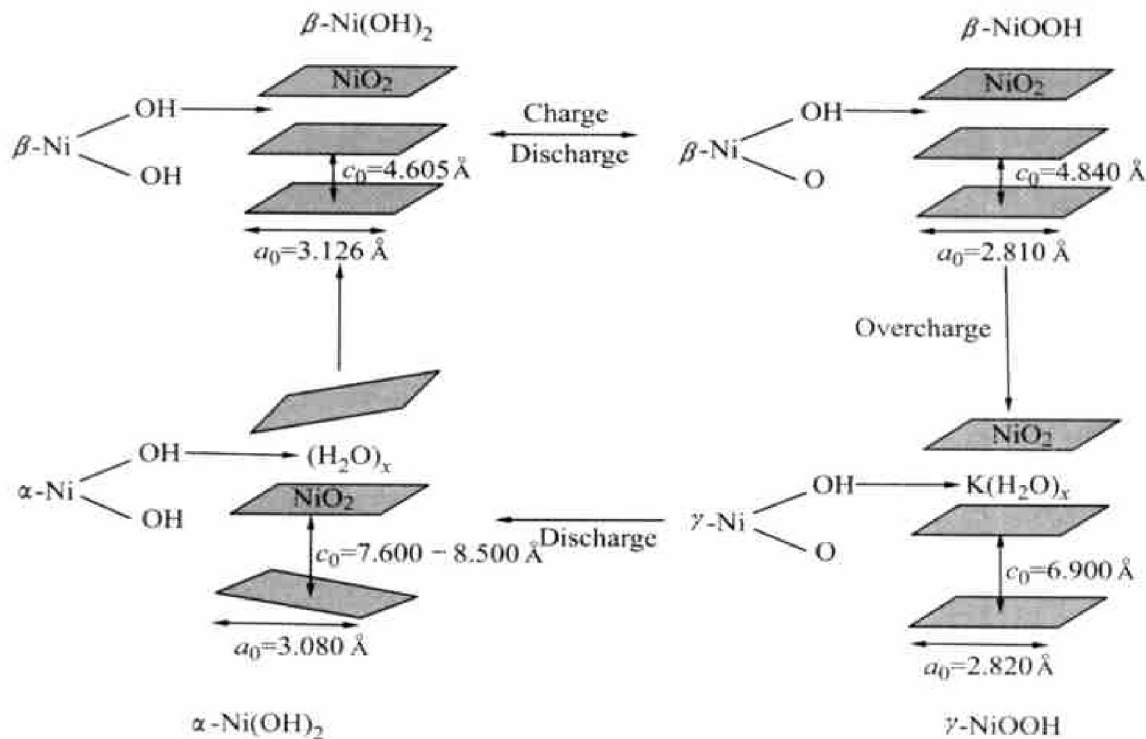


Fig. 9 Bode's representation of nickel hydroxides

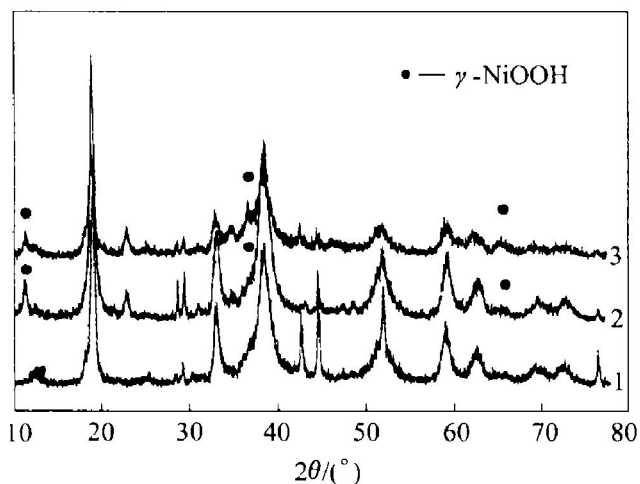


Fig. 10 XRD patterns of the positive electrodes after different charging-discharging cycles
1—Before cycle; 2—400 cycles; 3—900 cycles

phases nickel electrodes with $\beta\text{-Ni(OH)}_2$, $\beta\text{-NiOOH}$, $\gamma\text{-NiOOH}$ and $\alpha\text{-Ni(OH)}_2$ from Fig. 9. The $\gamma\text{-NiOOH}$ formation is associated with swelling or volume expansion of Ni electrodes. The phase change from $\beta\text{-Ni(OH)}_2$ to $\gamma\text{-NiOOH}$ can be correlated to 44% increasing in volume. Even at the discharge state, there exists $\gamma\text{-NiOOH}$ in the positive electrode^[11] (see Fig. 10).

The surface morphology of the negative electrodes is shown in Fig. 11. The alloy particles before charge-discharge cycling exhibit smooth surface with large size, but the alloy become rough and the particle size obviously decrease due to the pulverization after

degradation. After the charge-discharge cycling, lattice expansion and shrinkage occurred on hydrogen storage alloys because of absorption and desorption of hydrogen. Such changes result in the cracks formation in the cross-section of the electrode and the increase of internal stress. It had been shown qualitatively by Boonstra et al^[6] that the cycling stability of the AB_5 alloy electrodes was influenced strongly by the particle size or the specific surface area of the MH powder. The particle pulverization during charge-discharge cycling was identified as the main origin for deterioration of the negative electrode in nickel/metal hydride batteries.

The EDAX patterns of the negative electrode of Ni/MH batteries (a, b, c and d) are shown in Fig. 12. It is shown that the elemental distribution of the alloy surface layer was relatively uniform. However after degradation at different temperatures, the significant loss of Al on surfaces of the alloy could be observed. Corroded Al was entirely dissolved from the negative electrodes and trapped in the nickel hydroxide lattice within the positive electrodes to form the pyroaurite-like alpha phase^[12].

Furthermore, since the alloy powder was corroded in the sealed battery, an oxide layer (M(OH)_x) was formed on the surface of the negative electrodes^[11]. The hydroxides as insulator were used not only to prevent further corrosion of the negative electrode and decrease the decay of the cycle-life, but also to increase the resistance of the electrode and decrease the electrocatalytic activity.

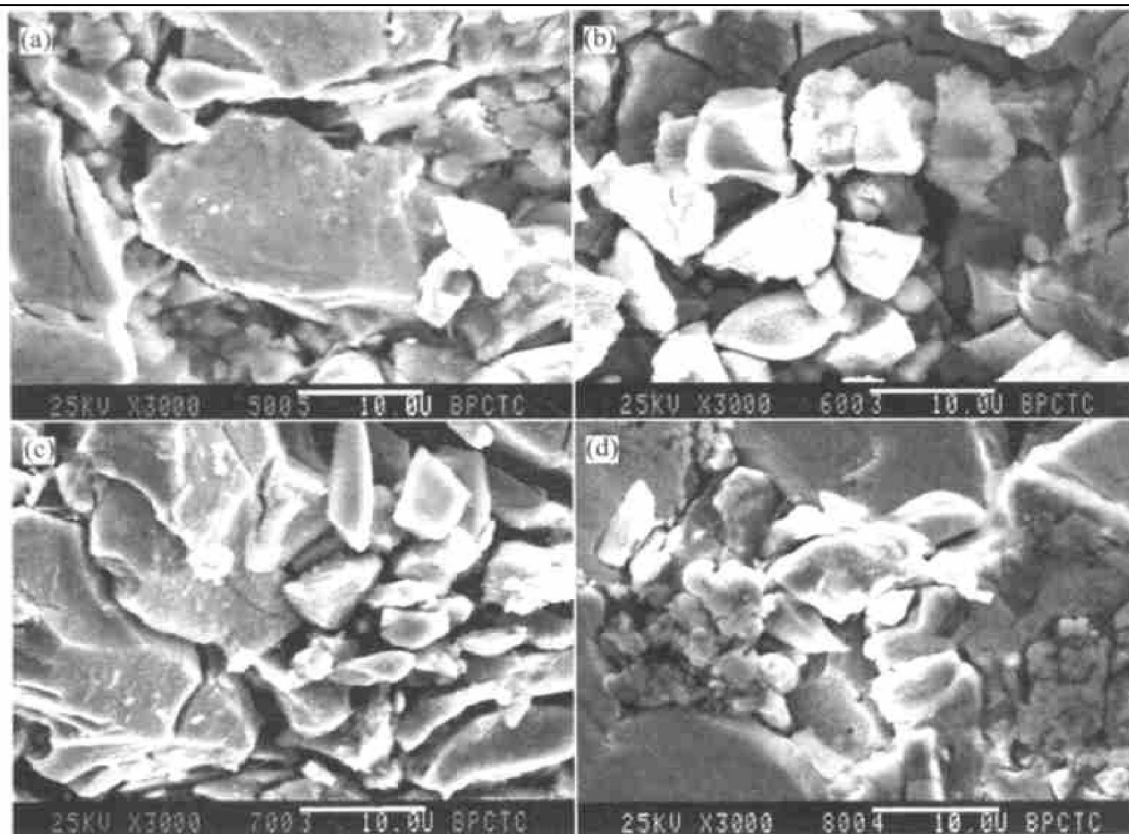


Fig. 11 SEM images of negative electrode

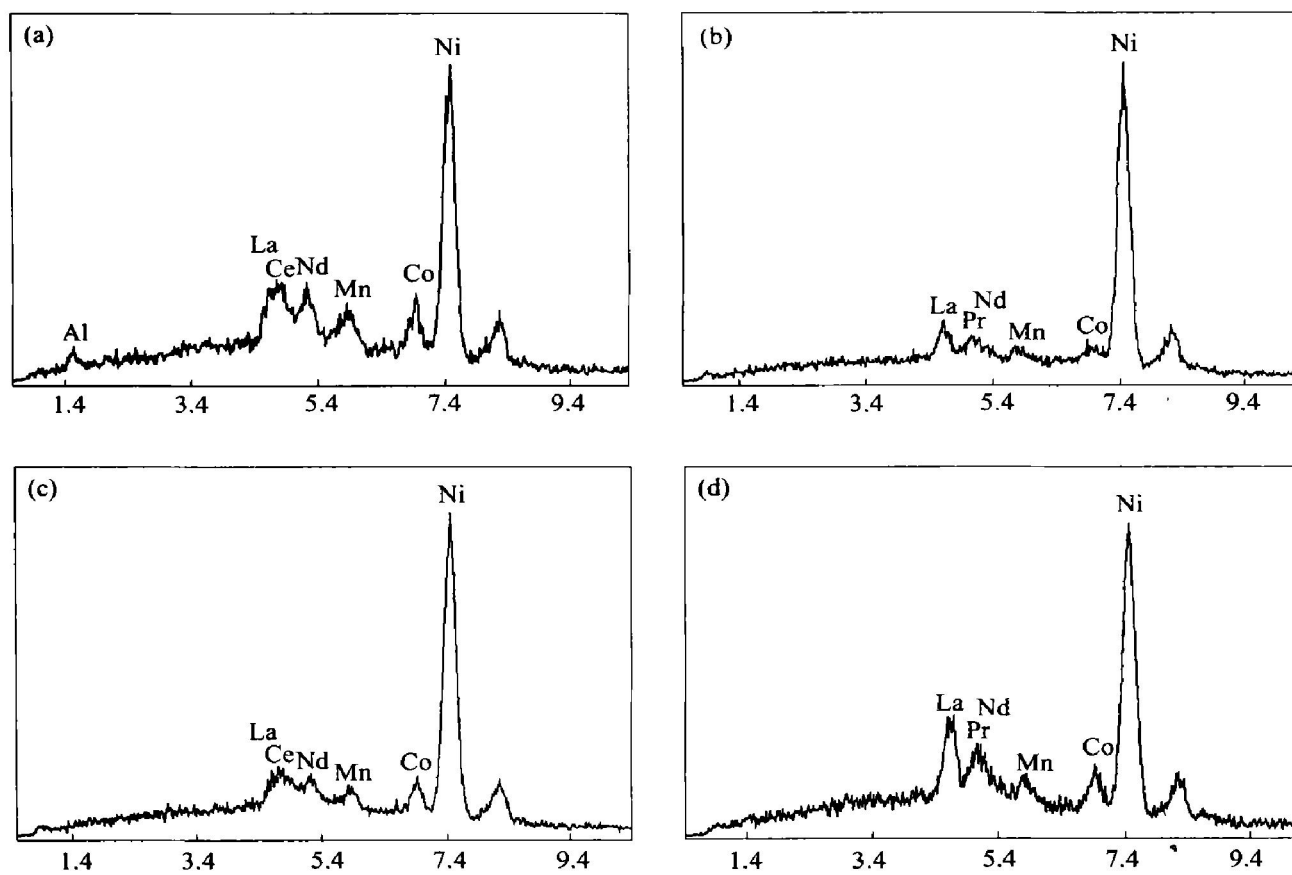


Fig. 12 EDAX patterns of negative electrode Ni/MH batteries

4 CONCLUSIONS

1) The decline rate of the D-size Ni/MH batter-

ies discharge capacity at $-20\text{ }^{\circ}\text{C}$ and $55\text{ }^{\circ}\text{C}$ are respectively 12.1% and 13.6%, the average discharge voltage decrease by a value of 0.13 V and 0.06 V.

Cycling stability of the Ni/MH battery is all declined obviously under unconventional conditions.

2) EIS results demonstrate that the increase of R_s , R_t and Z_w leads to the degradation of the performance of the nickel/metal hydride batteries.

3) SEM and EDAX results show that the particle pulverization, oxidation and irreversible structure change during charge/discharge are main origins that lead to the deterioration of the both electrodes in Ni/MH batteries.

4) The capacity degradation of Ni/MH batteries under low temperature is reversible, belonging to transient degradation. While that of high and normal temperatures are not reversible, belonging to permanent degradation.

Acknowledgments

The authors specially express thanks to Prof. Hong Cunmao for his experimental support and helpful comments.

REFERENCES

- [1] Soria M L, Chacón J, Hernández J C. Metal hydride electrodes and Ni/MH batteries for automotive high power applications[J]. *Journal of Power Sources*, 2001, 102(1): 97 - 104.
- [2] Akihiro T, Noriyuki F, Munehisa I, et al. Development of nickel/metal hydride batteries for Evs and HEVs[J]. *Journal of Power Sources*, 2001, 100(1): 117 - 124.
- [3] Nelson R F. Power requirements for batteries in hybrid electric vehicles[J]. *Journal of Power Sources*, 2000, 91(1): 2 - 26.
- [4] Tetsuo S, Ituki U, Hiroshi I. R&D on metal hydride materials and NiMH batteries in Japan[J]. *J Alloys and Compounds*, 1999, 293 - 295(3): 762 - 769.
- [5] Willems J J G, Buschow K H J. From permanent magnets to rechargeable hydride electrodes[J]. *Journal of the Less-Common Metals*, 1987, 129(1): 13 - 30.
- [6] Boonstra A H, Lippits G J M, Bernards T N M. Degradation processes in a LaNi_5 electrode[J]. *Journal of the Less-Common Metals*, 1989, 155(1): 119 - 131.
- [7] XIA Bao-jia, SHI Peng-fei, YIN Ge-ping, et al. Degradation mechanism of misch metal alloy hydride electrodes [J]. *J Alloys and Compounds*, 1999, 293 - 295(2): 737 - 741.
- [8] CHENG Sha-an, ZHANG Jiar-qing, LIU Hong, et al. Study of early cycling deterioration of a Ni/MH battery by electrochemical impedance spectroscopy[J]. *Journal of Power Sources*, 1998, 74(1): 155 - 157.
- [9] CHENG Sha-an, ZHANG Jiar-qing, ZHAO Mir-hua, et al. Electrochemical impedance spectroscopy study of Ni/MH batteries[J]. *J Alloys and Compounds*, 1999, 293 - 295(3): 814 - 820.
- [10] Zho Z Q, Lin G W, Zhang J L, et al. Degradation behavior of foamed nickel positive electrodes of NiMH batteries[J]. *J Alloys and Compounds*, 1999, 293 - 295(3): 795 - 798.
- [11] LI Li, WU Feng, YANG Kai. Degradation behavior of electrochemical performance of sealed-type nickel/metal hydride batteries[J]. *Journal of Rare Earths*, 2003, 21(3): 341 - 346.
- [12] Leblanc P, Jordy C, Knosp B, et al. Mechanism of alloy corrosion and consequences on sealed nickel metal hydride battery performance[J]. *J Electrochem Soc*, 1998, 145(3): 860 - 863.

(Edited by LI Yan-hong)